RSC Advances

ROYAL SOCIETY OF CHEMISTRY

www.rsc.org/advances

Room-temperature Phosphorescence by Mn-Doped ZnS Quantum Dots Hybrid with Fenton System for Selective Detection of Fe^{2+}

Qing Jin, Yueli Hu, Yuxiu Sun, Yan Li*, Jianzhong Huo, Xiaojun Zhao

Key Laboratory of Inorganic-Organic Hybrid Functional Material Chemistry, Ministry of Education, Tianjin Key Laboratory of Structure and Performance for Functional Molecule, College of Chemistry, Tianjin Normal University, Tianjin, 300387, P.R. China

* E-mail: nkliyan398@gmail.com

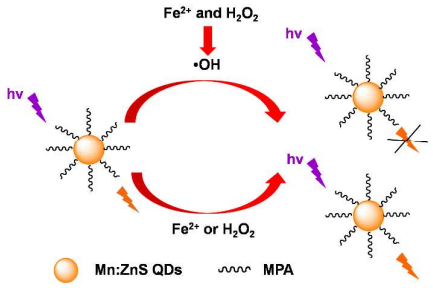

Fe^{2+} was selectively detected based on the phosphorescence quenching of MPA-Mn-ZnS QDs caused by hydroxyl radicals from Fenton reaction.

Room-temperature Phosphorescence by Mn-Doped ZnS Quantum Dots Hybrid with Fenton System for Selective Detection of Fe^{2+}

Qing Jin, Yueli Hu, Yuxiu Sun, Yan Li*, Jianzhong Huo, Xiaojun Zhao

Key Laboratory of Inorganic-Organic Hybrid Functional Material Chemistry, Ministry of Education, Tianjin Key Laboratory of Structure and Performance for Functional Molecule, College of Chemistry, Tianjin Normal University, Tianjin, 300387, P.R. China

* E-mail: nkliyan398@gmail.com

ABSTRACT

The phosphorescent 3-mercaptopropionic acid (MPA) capped Mn-doped ZnS quantum dots (MPA-Mn:ZnS QDs)-Fenton hybrid system was developed for highly sensitive detection of Fe^{2+} in environmental samples and biological fluids. The phosphorescence of the MPA-Mn:ZnS QDs can be effectively quenched by hydroxyl radicals produced from the Fenton reaction between Fe^{2+} and H_2O_2 at the low concentration level. But the phosphorescence of MPA-Mn:ZnS QDs can not be quenched by either Fe^{2+} or H_2O_2 each at the same concentration level. Thus, Fe^{2+} can be indirectly detected using the phosphorescence quenching caused by hydroxyl radicals based on the Fenton reaction. The possible mechanism for the quenching effect of Fe^{2+} was elucidated as electron transfer from the conduction band of MPA-Mn:ZnS QDs to the unoccupied band of hydroxyl radicals. The phosphorescent hybrid system allowed highly sensitive detection of Fe^{2+} in aqueous solution with a wide linear range of 0.01-10 μM and a detection limit of 3 nM, and the precision for 11 replicate detection of 0.1 μM Fe^{2+} was 1.5 % (relative standard deviation, RSD). The developed method was applied to determine Fe^{2+} in environmental samples and biological fluids with the quantitative spike recoveries from 95 % to 104 %.

Keywords: Room-temperature Phosphorescence; Mn-Doped ZnS Quantum Dots; Fenton reaction; sensitive detection of Fe^{2+}

Introduction

Many metals are considered essential trace elements and must be present in low concentrations in the human body for normal cellular function.[1-7] Iron is one of the most important elements and plays a central role in environmental and biological systems, owing to its easy redox reaction between Fe^{2+} and Fe^{3+}.[7-12] In environmental systems, Fe^{2+} is the most common form of iron element in the ground water and mineral water, and drinking mineral water is beneficial to the health of human body.[9] In biological systems, Fe^{2+} is predominantly high spin in aqueous biological environments, for example, ferrous heme can interact with molecular oxygen.[11-14] Thus, the discrimination and selective detection of Fe^{2+} has potential applications in the environment as well as in biological systems.

But to date, many methods for the quantitative detecting of Fe^{3+} have been developed by colorimetric method,[13] atomic absorption spectrometry,[15] voltammetry,[16] fluorescent probes [10,17-20] and so on,[21] detection of Fe^{2+} is paid poor attention by people for the instability. Recently, a colorimetric approach for selectively sensing Fe^{2+} ions was reported using CTAB-stabilized Au-Ag nanorods (CTAB-Au-Ag NRs) in the presence of poly(sodium 4-styrenesulfonate) (PSS).[22] This method can be utilized without complicated pretreatment, but most of the colorimetric probes suffer drawback in poor sensitivity. Moreover, a fluorescent nanoprobe method was reported for discrimination and sensitive detection of Fe^{2+} based on the fluorescence quenching of GSH-CdTe QDs.[23] Fluorescent probes have high photoluminescence efficiency, but the

CdTe QDs suffer drawbacks such as the potential toxicity from the toxic raw material Cd^{2+}, which hamper their application as promising optical labels in biological fluids for sensing.[24,25] So, it is necessary to develop some environmental friendly methods for discrimination of different iron species and sensitive detection of Fe^{2+} in virtue of sensitivity and convenience.

Recently, room-temperature phosphorescence (RTP) detection has attracted much attention due to its many advantages, such as the wider gap between the excitation and emission spectra, the longer emission lifetime, anti-interference from autofluorescence and the scattering light of the matrix.[26,27] The selectivity is also enhanced because phosphorescence is less common than fluorescence.[28] It is widely studied for developing sensors with great success, thus becoming a hotpot.[27,29-34] A series of RTP method based on the phosphorescence property of the Mn-doped ZnS QDs have been reported for the detection of enoxacin in biological fluids, [27] glucose in serum samples,[30] acetone in natural water,[31] heparin in human serum[33] and selective determination of catechol from organic isomers.[29] However, to our knowledge, QDs based RTP probes for discrimination of different iron species and sensitive detection of Fe^{2+} at trace level in environmental samples and biological fluids have not been reported before.

Here, the MPA-Mn:ZnS QDs-Fenton hybrid system is explored to develop a RTP method for the facile, sensitive, and selective detection of Fe^{2+} in environmental samples and biological fluids. Firstly, different metal species (Fe^{2+} and Fe^{3+}) can be discriminated by the different quenching kinetics of MPA-Mn:ZnS QDs. Moreover,

Fe^{2+} can be sensitively and indirectly detected using the phosphorescence quenching effect of enlargement caused by hydroxyl radicals, which are produced from the Fenton reaction between the low concentration of Fe^{2+} and H_2O_2.[35,36] Likewise, the hydroxyl radicals lead to the phosphorescence quenching of MPA-Mn:ZnS QDs due to the electron transfer from the conduction band of QDs to the unoccupied band of hydroxyl radicals, allowing highly selective and sensitive detection of Fe^{2+} in aqueous solution with a detection limit of 3 nM.

Experimental section

Reagents

All reagents used were at least of analytical grade. $ZnSO_4 \cdot 7H_2O$, $Mn(CH_3COO)_2 \cdot 4H_2O$, $Na_2S \cdot 9H_2O$, ascorbic acid, Tris-HCl buffer solution (10 mM of Tris, pH 7.4) were purchased from Tianjin Guangfu Fine Chemical Research Institute. 3-mercaptopropionic acid (MPA, 99 %) was obtained from Beijing J&K Chemical Co., Ltd. H_2O_2 (30 %) was from Tianjin Benchmark Chemical Reagent Co., Ltd. Ultrapure water was obtained from Wahaha company. Aqueous solutions of Fe^{2+}, Fe^{3+}, K^+, Na^+, Ca^{2+}, Mg^{2+}, Al^{3+}, Mn^{2+}, Co^{2+}, Ni^{2+}, Cu^{2+}, and Zn^{2+} were prepared from $FeSO_4 \cdot 7H_2O$, $FeCl_3 \cdot 6H_2O$, KCl, NaCl, $CaCl_2 \cdot 4H_2O$, $MgCl_2 \cdot 6H_2O$, $AlCl_3 \cdot 9H_2O$, $MnCl_2$ $4H_2O$, $CoCl_2 \cdot 6H_2O$, $NiCl_2 \cdot 6H_2O$, $CuCl_2 \cdot 2H_2O$ and $ZnCl_2 \cdot 7H_2O$, respectively. These reagents were purchased from Tianjin Kewei Co., Ltd .

Apparatus

The RTP measurements were performed on a Cary Eclipse Fluorescence

spectrophotometer (Agilent Technologies) equipped with a plotter unit and a quartz cell (1 cm × 1 cm) in the phosphorescence mode. The phosphorescent emission spectra were recorded in the wavelength range of 500-700 nm upon excitation at 316 nm. The slit width of excitation and emission was 10 and 20 nm, respectively. The photomultiplier tube (PMT) voltage was set at 700 V. Absorption spectra were recorded on an Ocean Optics DH-2000-BAL UV-VIS-NIR LIGHTSOURCE. The Fourier transform infrared (FT-IR) spectra (4000−400 cm^{-1}) were recorded using a NICOLET 6700 FT-IR spectroscope with KBr pellets. The transmission electron microscopy (TEM) on a Tecnai G2 F20 (FEI) was operated at a 200 kV accelerating voltage. The samples for TEM were obtained by drying sample droplets from Tris-HCl (pH 7.4, 10 mM) dispersion onto a 300-mesh Cu grid coated with a carbon film. The X-ray diffraction (XRD) spectra were collected on a Bruker D8 diffractometer at a scanning rate of 1° min^{-1} in the 2θ range from 5 to 80º. The X-ray photoelectron spectroscopy (XPS) measurements were carried out on a Kratos Axis Ultra DLD spectrometer fitted with a monochromated Al KR X-ray source (hν = 1486.6 eV), hybrid (magnetic/electrostatic) optics, and a multichannel plate and delay line detector. The Zeta potential was measured by Malvern Zetasizer Nano ZS (red badge) with 633 nm He-Ne laser. Seven samples' composition quantitative analysis of Fe^{2+} was analyzed on the X7 Series Inductively coupled plasma mass spectrometry (ICP-MS) (Thermo Electron Corporation).

Synthesis of the Mn-Doped ZnS QDs

Mn-doped ZnS QDs were synthesized in an aqueous solution using MPA as a

stabilizer on the basis of a published procedure with minor modification.[27] 50 mL of 0.04 M MPA, 5 mL of 0.1 M $ZnSO_4$, and 5 mL of 0.01 M $Mn(CH_3COO)_2 \cdot 4H_2O$ were added to a three-necked flask. The mixture was adjusted to pH 11 with 1 M NaOH and stirred under nitrogen at room temperature for 30 min. Then 5 mL of 0.1 M Na_2S was quickly injected into the solution. After stirring for 20 min, the solution was aged at 50 °C under air for 2 h to form MPA-Mn:ZnS QDs. These QDs were precipitated with ethanol, separated by centrifuging, and dried in vacuum. The highly soluble MPA-Mn:ZnS QDs were obtained.

Phosphorescence Experiments

For discrimination of Fe^{2+} and Fe^{3+}, 150 μL of 200 mg L^{-1} MPA-Mn:ZnS QDs, 1 mL of 0.1 M Tris-HCl buffer solution (pH 7.4), and 2 mL of 5 μM Fe^{2+} or Fe^{3+} standard solution were added to a 10 mL calibrated test tube. Fe^{2+} was prepared by $FeSO_4 \cdot 7H_2O$ in ultrapure water just prior to use. The mixture was diluted to volume with ultrapure water, mixed thoroughly, and immediately scanned by Cary Eclipse Fluorescence spectrophotometer. The phosphorescence intensity was recorded every 1 min for a total time of 20 min to observe their quenching kinetics.

For determination of Fe^{2+}, 150 μL of 200 mg L^{-1} MPA-Mn:ZnS QDs, 1 mL of 0.1 M Tris-HCl buffer solution (pH 7.4), 500 μL of 10 μM H_2O_2, and 2 mL of 0.5 μM Fe^{2+} standard solution or 2 mL of real samples (water samples or biological fluid samples) were added to a 10 mL calibrated test tube. Fe^{2+} was prepared by $FeSO_4 \cdot 7H_2O$ in ultrapure water just prior to use.The mixture was diluted to volume with ultrapure water, mixed thoroughly, and 10 minutes later scanned by Cary Eclipse Fluorescence

spectrophotometer. The phosphorescence spectra of MPA-Mn:ZnS QDs were recorded upon excitation at 316 nm. The phosphorescence intensity at the maximum phosphorescence wavelength was used for quantification.

Environmental Samples and Biological Fluid Samples

Two tap water, three river water and two mineral water samples were collected locally. All water samples were filtered through 0.22 μm filters, and analyzed immediately after sampling. For analysis, all water samples were subjected to 5-fold dilution, respectively.

Fresh human urine and serum samples were collected from healthy young volunteers treated in the local hospital. Each urine sample was centrifuged at 10000 rpm for 10 min to remove particulate matter and the supernatants were used and diluted 100 times, with Tris-HCl buffer solution (pH 7.4) before analysis. Each serum sample was centrifuged at 14000 rpm for 10 min to remove the part of deposition to eliminate the possible interference of proteins in human serum and the supernatants were used and diluted 100 times, with Tris-HCl buffer solution (pH 7.4) before analysis.

Results and discussion

Characterization of the MPA-Mn:ZnS QDs

MPA-Mn:ZnS QDs were prepared based on a previously published method with minor modification.[27] Fig. 1A showed the phosphorescence intensity of MPA-Mn:ZnS QDs gradually increased as its concentration increased and it had a good liner relationship in a large concentration range of 1-13 mg L^{-1} (Fig. S1). It was also

indicating the good solvent dispersibility of MPA-Mn:ZnS QDs in aqueous solution. The TEM image (Fig. 1B) of the prepared MPA-Mn:ZnS QDs were quasi-spherical shape and almost uniform size in diameter about 3.5 nm. The crystal lattice was clearly visible from the inset (Fig. 1B). Further information on the structure of the as-prepared MPA-Mn:ZnS QDs was obtained from the selected area electron diffraction pattern (inset of Fig. 1C). The selected area electron diffraction pattern exhibits broad diffuse rings typical of particles. The (111), (220) and (311) planes were indexed confirming the cubic phase. This result agreed well with that powder XRD pattern (Fig. 1C). The presence of three characteristic diffraction peaks in XRD pattern was also demonstrated that the lattice structure of the MPA-Mn:ZnS QDs was close to a cubic zinc blende structure. The FT-IR spectra of the MPA-Mn:ZnS QDs and pure MPA were compared to examine the MPA capping on the surface of Mn:ZnS QDs (Fig. 1D). It was depicted that the sulfhydryl band at 2570 cm^{-1} disappeared, the carboxyl group stretching band shifted from 1710 cm^{-1} to 1545 cm^{-1}, and the free hydroxyl groups band at 3000 cm^{-1} of MPA shifted to 3400 cm^{-1}. These results indicated that MPA had been successfully capped onto the surface of Mn:ZnS QDs by the sulfhydryl functionality.

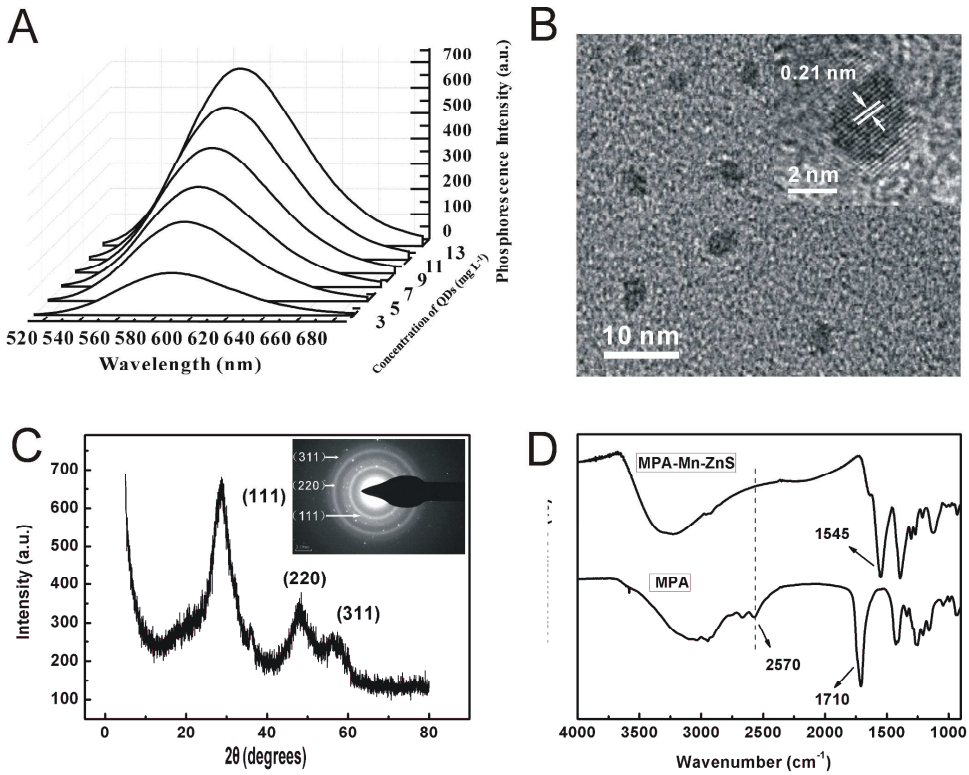

Fig. 1 (A) the concentration-dependent phosphorescence spectra of MPA-Mn:ZnS QDs; (B) TEM image of MPA-Mn:ZnS QDs; (C) XRD pattern and selected area electron diffraction pattern of MPA-Mn:ZnS QDs; (D) the FT-IR spectra of the MPA-Mn:ZnS QDs and pure MPA.

Phosphorescence characteristics of the as-prepared MPA-Mn:ZnS QDs were illustrated in Fig. 2. An absorption peak at about 300 nm appeared in the absorption spectrum of the MPA-Mn:ZnS QDs (Fig. 2, curve a). No phosphorescence was emitted from the MPA-Mn:ZnS QDs before aging (Fig. 2, curve c), but strong phosphorescence emission was shown at 588 nm when the QDs were excited at 316 nm after aging at 50 °C for 2 h (Fig. 2, curve b). In addition, without Mn doping, the ZnS QDs showed no phosphorescence emission.[27] The phosphorescence lifetime of the prepared MPA-Mn:ZnS QDs was evaluated to be 2 ms from the decay curve of the

phosphorescence emission (inset of Fig. 2). The observed phosphorescence was attributed to the transition of Mn^{2+} from the triplet state ($^4T_1$) to the ground state ($^6A_1$).[37]

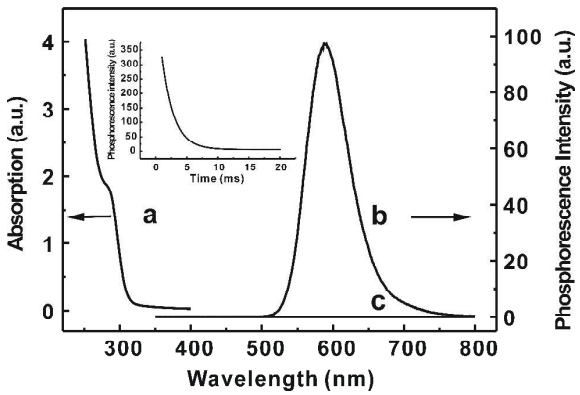

Fig. 2 Absorption spectrum of MPA-Mn:ZnS QDs after aging at 50 °C (curve a) and RTP spectra of MPA-Mn:ZnS QDs after and before aging at 50 °C (curve b, c). The inset showed the decay curve of phosphorescence lifetime of MPA-Mn:ZnS QDs aged at 50 °C.

The strategy for RTP detection of Fe^{2+} based on the MPA-Mn:ZnS QDs-Fenton Reaction hybrid system

It is well-known that Fe^{2+} has been found to react with H_2O_2 to produce the extremely reactive hydroxyl radicals, the so-called Fenton Reaction.[35,36,38] In this paper, we can indirectly detect Fe^{2+} by investigating the quenching effect of enlargement caused by hydroxyl radicals on the phosphorescence of MPA-Mn:ZnS QDs. To investigate Fe^{2+}-based Fenton Reaction on MPA-Mn:ZnS QDs, the concentrations of Fe^{2+} and H_2O_2 were set at very low levels to ensure that individual Fe^{2+} or H_2O_2 had negligible influence on the phosphorescence intensity of MPA-Mn:ZnS QDs (Fig. 3A, curve b and c). The generated hydroxyl radicals from the mixture of Fe^{2+} and H_2O_2

were observed to quench the phosphorescence of MPA-Mn:ZnS QDs to a much larger extent than individual Fe^{2+} or H_2O_2 (Fig. 3A, curve d). But Fe^{3+} and H_2O_2 could not have the same phenomenon by the same operation (Fig. S2).

It was necessary to reduce the interference of Fe^{3+} before the detection of Fe^{2+}. Interestingly, the phosphorescence quenching of MPA-Mn:ZnS QDs exhibited different responses to Fe^{2+} and Fe^{3+}. The time course of the phosphorescence of the MPA-Mn:ZnS QDs in the high concentration of Fe^{3+} or Fe^{2+} was illustrated in Fig. S3. The phosphorescence was quenched by about 6.5 % in 10 min by 1 μM Fe^{2+}, and remained unchanged with further increasing reaction time, indicating a quenching equilibrium had been reached. In contrast, the phosphorescence intensity almost did not decrease in the total 20 min after the addition of 1 μM Fe^{3+}. Moreover, we detected the effect of capping agents for the Mn:ZnS QDs on the quenching behavior of Fe^{2+} and Fe^{3+} by thioglycolic acid (Fig. S4). The results showed that the quenching behavior of Fe^{2+} and Fe^{3+} were not affected by different capping agents. It was also indicated that Fe^{2+} was stable at least within 10 min. Thus, the interference from Fe^{3+} can be reduced as low as possible in the selectively detection of Fe^{2+}.

Molecular logic gates from Fe^{2+}-based Fenton Reaction on MPA-Mn:ZnS QDs

We designed a molecular logic gates which used the concept of logic gate to validate the strategy for selective detection of Fe^{2+} based on the MPA-Mn:ZnS QDs-Fenton Reaction hybrid system. Molecular logic gates (AND, OR，NAND, etc.) distinguish analytes through different signal outputs (particularly, optical responses) upon changing inputs.[39,40] The logic gate employed Fe^{3+}, Fe^{2+} and H_2O_2 as the three inputs,

and the phosphorescence quenching efficiency of MPA-Mn:ZnS QDs was defined as the output. With respect to inputs, the presence and absence of Fe^{3+}, Fe^{2+} and H_2O_2 were defined as ‘‘1’’ and ‘‘0’’, respectively. Additionally, we defined the phosphorescence quenching and unchanged phosphorescence as outputs ‘‘1’’ and ‘‘0’’, respectively. Fig. 3B showed the characteristics of MPA-Mn:ZnS logic gate by observing the phosphorescence responses under eight possible input conditions. It was found that there were only two input conditions-(011) and (111)- would induce the phosphorescence quenching (output 1). Thus, the MPA-Mn:ZnS QDs-Fenton reaction hybrid system could be used to selectively detect Fe^{2+} because the phosphorescence quenching of MPA-Mn:ZnS QDs exhibited different responses to Fe^{2+} and Fe^{3+}.

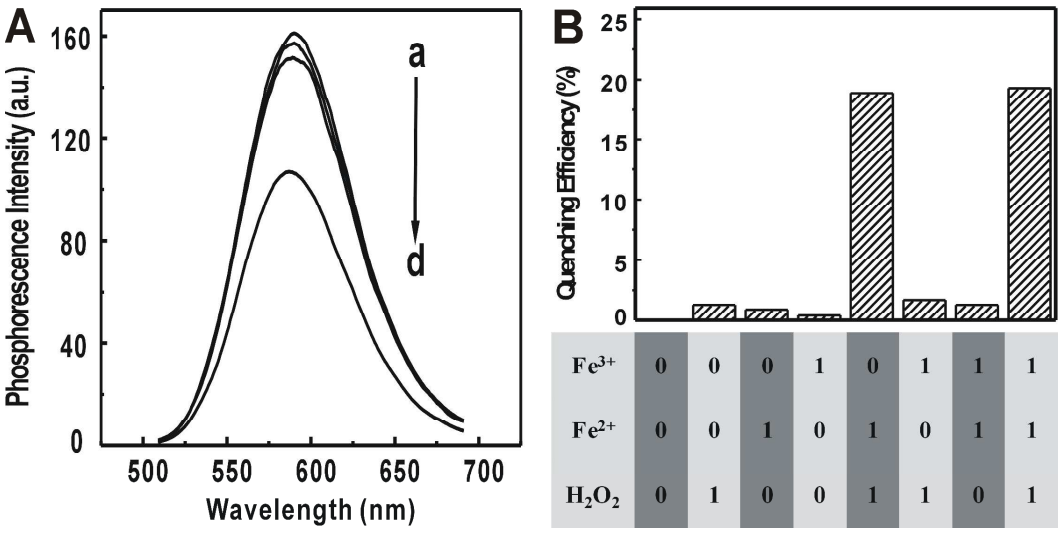

Fig. 3 (A) Phosphorescence spectra of MPA-Mn:ZnS QDs (3 mg L^{-1}): (a) in the absence of Fe^{2+} and H_2O_2; (b) 10 min after addition of 0.1 μM Fe^{2+}; (c) 10 min after addition of 0.5 μM H_2O_2; (d) 10 min after addition of 0.1 μM Fe^{2+} and 0.5 μM H_2O_2. (B) The phosphorescence quenching efficiencies of the MPA-Mn:ZnS logic gate under eight input-conditions. The concentrations of Fe^{2+} and Fe^{3+} were 0.1 μM and the

concentration of H_2O_2 was 0.5 μM. All measurements were carried out in Tris-HCl buffer solution (pH 7.4, 10 mM).

Factors Affecting the Sensitivity of the MPA-Mn:ZnS QDs-Fenton Reaction Hybrid System for RTP Detection of Fe^{2+}

Fig. 4A showed that the enhancement of the phosphorescence intensity of MPA-Mn:ZnS QDs was proportional with increasing of the concentration of MPA-Mn:ZnS QDs. Simultaneously, the quenching efficiency of MPA-Mn:ZnS QDs in the presence of 0.1 μM Fe^{2+} and 0.5 μM H_2O_2 decreased rapidly with increasing of the concentration of MPA-Mn:ZnS QDs. Considering the phosphorescence intensity and quenching efficiency, 3 mg L^{-1} of MPA-Mn:ZnS QDs were used in the further detection process.

The effect of pH-dependent phosphorescence quenching efficiency of 3 mg L^{-1} MPA-Mn:ZnS QDs was tested with 0.1 μM Fe^{2+} and 0.5 μM H_2O_2. As the MPA-Mn:ZnS QDs were unstable in acidic media, pH lower than 6 was not considered. In the studied pH range of 6.0-7.4, the quenching efficiency of the MPA-Mn:ZnS QDs gradually increased in the presence of Fe^{2+} and H_2O_2. In contrast, it gradually decreased in the studied pH range of 7.4-9.5 (Fig. 4B). To keep the MPA-Mn:ZnS QDs as stable as possible and to ensure highly sensitive detection of Fe^{2+}, Tris-HCl buffer solution (pH 7.4, 10 mM) was used.

The effect of Fe^{2+}-concentration dependent phosphorescence quenching efficiency of 3 mg L^{-1} MPA-Mn:ZnS QDs was tested without H_2O_2 in Tris-HCl (pH 7.4, 10mM, Fig. 4C). The concentration of Fe^{2+} was set at very low levels to ensure that individual

Fe^{2+} caused negligible influence on the phosphorescence intensity of MPA-Mn:ZnS QDs. Therefore, 0.1 μM of Fe^{2+} solution was determined as the optimum detecting concentration.

The effect of H_2O_2-concentration dependent phosphorescence quenching efficiency of 3 mg L^{-1} MPA-Mn:ZnS QDs was tested with 0.1 μM Fe^{2+} in Tris-HCl (pH 7.4, 10mM). There was no obvious change of phosphorescence quenching efficiency of MPA-Mn:ZnS QDs in the studied H_2O_2 concentration range of 0.1-10 μM (Fig. 4D). The concentration of H_2O_2 higher than 10 μM was not tested because H_2O_2 can individually cause quenching of MPA-Mn:ZnS QDs. Therefore, 0.5 μM of H_2O_2 solution was employed in the detection process.

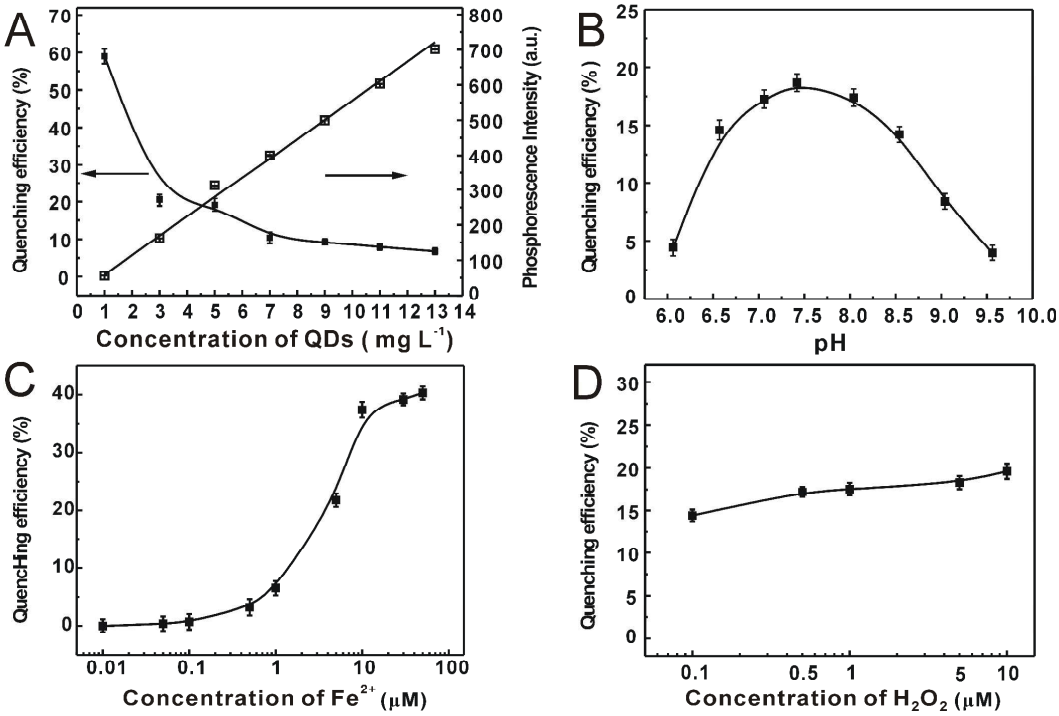

Fig. 4 (A) Quenching efficiency in the presence of 0.1 μM Fe^{2+} and 0.5 μM H_2O_2 against the concentration of MPA-Mn:ZnS QDs, and the phosphorescence evolution with the concentration of MPA-Mn:ZnS QDs in the absence of Fe^{2+} and H_2O_2. (B) pH-dependent

phosphorescence quenching efficiency of 3 mg L^{-1} MPA-Mn:ZnS QDs in the presence of 0.1 μM Fe^{2+} and 0.5 μM H_2O_2. (C) Fe^{2+}-concentration dependent phosphorescence quenching efficiency of 3 mg L^{-1} MPA-Mn:ZnS QDs in the absence of H_2O_2. (D) H_2O_2-concentration dependent phosphorescence quenching efficiency of 3 mg L^{-1} MPA-Mn:ZnS QDs in the presence of 0.1 μM Fe^{2+}. All measurements were carried out in Tris-HCl buffer solution (pH 7.4, 10 mM).

Selectivity of the MPA-Mn:ZnS QDs-Fenton Reaction hybrid system for RTP Detection of Fe^{2+}

To show the potential application of MPA-Mn:ZnS QDs-Fenton hybrid system for detecting Fe^{2+}, the phosphorescence responses of MPA-Mn:ZnS QDs toward K^+, Na^+, Ca^{2+}, Mg^{2+}, Al^{3+}, Zn^{2+}, Ni^{2+}, Mn^{2+}, Co^{2+}, Fe^{3+}, Cu^{2+}, and Fe^{2+} in the presence of 0.5 μM H_2O_2 were studied (Fig. S5). The results showed that only Fe^{2+} gave significant phosphorescence quenching effect of MPA-Mn:ZnS QDs, indicating the high selectivity of MPA-Mn:ZnS QDs-Fenton hybrid system for the detection and specific recognition of Fe^{2+} in aqueous solution.

Further experiments for the effect of various co-existing metal cations and some anions on the phosphorescence quenching of MPA-Mn:ZnS QDs (3 mg L^{-1}) by 0.1 μM Fe^{2+} in the presence of 0.5 μM H_2O_2 were examined to show high anti-interference from other co-existing ions for detecting Fe^{2+} (Table 1). The phosphorescence quenching of MPA-Mn:ZnS QDs (3 mg L^{-1}) by 0.1 μM Fe^{2+} was unaffected (An error of ±3.0 % in the relative phosphorescence intensity was considered tolerable) by 1 mM of K^+ and Na^+, 400 μM of Ca^{2+} and Mg^{2+}, 5 μM of Al^{3+}, 1 μM of $Fe^{3+}$and Zn^{2+}, 0.2μM

of $Mn^{2+}$and Cu^{2+}, 0.1μM of Co^{2+}, 0.05 μM of Ni^{2+}, Hg^{2+} and Cr^{3+}, 600 μM of SO_4^{2-}, 1 mM of Cl^-. The tolerant concentrations for transition metal ions were much lower than those of alkali and alkali-earth metal ions. For example, transition metal ions, such as Mn^{2+}, Ni^{2+}, and Co^{2+}, can also participate in "Fenton-like" reactions, but their ability to induce the generation of hydroxyl radical was much lower than that of Fe^{2+}.[41] As the average concentrations of these co-existing metal ions in a river water matrix did not exceed the tolerant concentrations (Table S1),[42] most potential interferences from these co-existing ions in river water samples can be eliminated by simple dilution for the detection of Fe^{2+}.

Table 1 Effect of Co-Existing Ions on the Detection of 0.1 μM Fe^{2+} by the Proposed QDs-Fenton Hybrid System Based Phosphorescence Probe

Metal ion	Concentration/μM	Quenched phosphorescence change/ %
K^+	1000	+1.1
Na^+	1000	-2.4
Ca^{2+}	400	-0.7
Mg^{2+}	400	-0.4
Al^{3+}	5	-1.8
Zn^{2+}	1	+2.5
Ni^{2+}	0.05	+1.7
Mn^{2+}	0.2	+1.2
Co^{2+}	0.1	+1.9
Fe^{3+}	1	+2.3
Hg^{2+}	0.05	+2.3
Cr^{3+}	0.05	+1.6

Figures of Merit for the MPA-Mn:ZnS QDs-Fenton Reaction Hybrid System for RTP Detection of Fe^{2+}

The phosphorescence quenching process can be described by the Stern-Volmer equation (Fig. 5):[43]

$$P_0 / P = 1 + K_{SV} C$$

where the P_0 and P are the phosphorescence intensity of the MPA-Mn:ZnS QDs in the absence and in the presence of analyte, respectively, K_{SV} is the Stern-Volmer quenching constant, which is related to the quenching efficiency, and C is the concentration of analyte. Fig. 5A showed the phosphorescence intensity of MPA-Mn:ZnS QDs gradually quenched as the concentration of Fe^{2+} increased, and the Fig. 5B gave the Stern-Volmer plots for Fe^{2+}. The P_0 / P of MPA-Mn:ZnS QDs had a good linear relationship to the concentration of Fe^{2+} (R^2 = 0.991) in the concentration range of 0.01−10 μM Fe^{2+} (Fig. 5B). Likewise, the linear regression equation was P_0 / P = 0.553C + 1.15 (where C is the concentration of Fe^{2+} in μM). The relative standard deviation (RSD) for 11 replicate detections of 0.1 μM Fe^{2+} was 1.5 %, showing the high precision for detecting Fe^{2+}. Moreover, the MPA-Mn:ZnS QDs-Fenton hybrid system also gave a low detection limit (3σ) of 3 nM for Fe^{2+}, which was comparable to or better than those obtained by other measures for different iron species (Table 2).

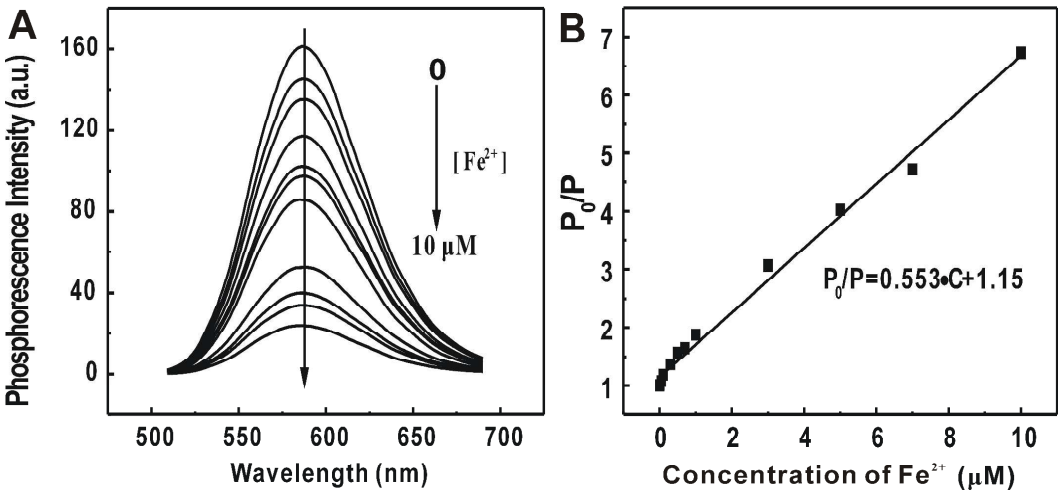

Fig. 5 (A) Effect of the concentration of Fe^{2+} on the phosphorescence spectra of MPA-Mn:ZnS QDs (3 mg L^{-1}) in the presence of 0.5 μM H_2O_2. (B) The Stern-Volmer plot for the phosphorescence quenching of the QDs by Fe^{2+} in the presence of 0.5 μM H_2O_2.

Table 2 Comparison of the Analytical Performance of the Sensing Systems for detection of Fe^{2+}

materials	linear range(μM)	detection limits(nM)	reference
CTAB-Au-Ag NRs	1-15	1000	22
CdTe QDs	0.01-1	5	23
$CePO_4:Tb^{3+}$	0.003-2	2	44
MOF-253	5–100	500	45
DNA–GO	0.01-1	2.4	46
MPA-Mn:ZnS QDs	0.01-10	3	this work

Possible Mechanism of the MPA-Mn:ZnS QDs-Fenton Reaction Hybrid System for RTP Detection of Fe^{2+}

It is well-known that Fe^{2+} has been found to react with H_2O_2 to produce the extremely reactive hydroxyl radicals, the so-called Fenton Reaction.[35,36,38]

$$Fe^{2+} + H_2O_2 \rightarrow Fe^{3+} + OH^- + \bullet OH$$

The hydroxyl radical (•OH) is a kind of reactive oxygen species which has an extremely strong ability to capture electrons, and •OH is also an efficient optics quencher. In order to further confirm that the quenching effect of enlargement was caused by •OH, ascorbic acid (Vc) (a kind of free radical scavenger) was added before and after the interaction between Fenton hybrid system and MPA-Mn:ZnS QDs (Fig. S6). Firstly, the concentration of Vc was set at very low levels (0.5 μM) to ensure that individual Vc caused negligible influence on the phosphorescence intensity of MPA-Mn:ZnS QDs (Fig. S6, curve a). Then, the effect of phosphorescence quenching of MPA-Mn:ZnS QDs weakened gradually (Fig. S6, curve b versus d). Therefore, Fenton hybrid system quenching effect came from •OH to MPA-Mn:ZnS QDs.

Moreover, •OH is an important active oxygen-containing species with a redox potential of 2.8 V (vs standard hydrogen electrode, SHE), and has extremely strong ability to capture electron（Fig. S7）.[47] The redox potential of the MPA-Mn:ZnS QDs measured by zeta was -1.68 V. Thus, It may have an electron transfer from the conduction band of MPA-Mn:ZnS QDs to the unoccupied band of •OH.

To understand the quenching of •OH mechanism better, two samples were prepared for the analysis by XPS (Fig. S8), curve a and curve b for MPA-Mn:ZnS QDs in the absence and presence of Fe^{2+} (5 μM) and H_2O_2 (25 μM), respectively. The inspection of the S 2p spectral region indicated that after addition of Fe^{2+} and H_2O_2, a new valence state of sulfur appeared on the surface (Fig. S8, curve b), with S 2p binding energy of about 168 eV. The new peak was attributed to the S(VI) in sulfite.[48]

Therefore, It may show that part S on the surface of the MPA-Mn:ZnS QDs was oxidized to the S (VI), for the electron transfer from the conduction band of MPA-Mn:ZnS QDs to the unoccupied band of •OH.

Application of the MPA-Mn:ZnS QDs-Fenton Reaction Hybrid System for the Determination of Fe^{2+} in Environmental Samples and Biological Fluids

The high selectivity and sensitivity made MPA-Mn:ZnS QDs-Fenton hybrid system promising for detecting Fe^{2+} in environmental samples and biological fluids. In environment samples, two samples from the tap, three samples from local rivers and two bottled mineral water samples were collected for the detection. As shown in Table 3, the quantitative spike-recoveries for detecting Fe^{2+} in real water samples ranged from 95 % to 104 %. In biological fluids, two samples from fresh human urine and three samples from human serum were collected for the detection. As shown in Table 4, the quantitative spike-recoveries for detecting Fe^{2+} in biological fluids ranged from 95 % to 102 %. In addition, the analytical results for Fe^{2+} in environmental samples and biological fluids obtained by the proposed method were in good agreement with those obtained by a flow injection inductively coupled plasma mass spectrometry (ICP-MS) method.[49] The operating conditions on flow injection ICP-MS were shown in Table S2. The above results demonstrated the accuracy of the QDs-Fenton hybrid system for selective detection of Fe^{2+} in environmental samples and biological fluids.

Table 3 Analytical Results for the Determination of Fe^{2+} in environmental samples

Sample	found by this method (mean ± σ, n = 3)/μM	recovery(mean ± σ, n = 3)[b]/ %	found by ICP-MS[49] (mean ± σ, n = 3)/μM

tap water 1	0.119±0.013	97±5	0.136±0.028
tap water 2	0.143±0.040	102±3	0.154±0.033
river water 1	nd[a]	99±4	nd
river water 2	nd	95±5	nd
river water 3	nd	104±3	nd
mineral water 1	nd	98±3	nd
mineral water 2	nd	96±4	nd

[a] nd: not detected. [b] For 0.20 μM Fe^{2+} spiked in environmental samples.

Table 4 Analytical Results (mean ± σ, n = 3) for the Determination of Fe^{2+} in biological fluids

Sample	Fe^{2+} in samples /μM	Fe^{2+} Spiked /μM	Fe^{2+} found /μM	recovery /%
Urine-1	nd[a]	0.1	0.094±0.017	95±3
Urine-2	nd	0.5	0.496±0.009	97±4
human serum-1	nd	0.1	0.078±0.012	96±4
human serum-2	nd	0.5	0.509±0.005	102±5
human serum-3	nd	1	0.985±0.003	99±2

[a] nd: not detected.

Conclusions

In this paper, MPA-Mn:ZnS QDs-Fenton hybrid system was developed for highly sensitive determination of Fe^{2+} based on the phosphorescence quenching effect of enlargement caused by hydroxyl radicals that produced from the Fenton reaction. The phosphorescence quenching of MPA-Mn:ZnS QDs exhibited different responses to Fe^{2+} and Fe^{3+}, which was applied for discrimination of different iron species and selective detection of Fe^{2+} at the nanomolar level. The Mn:ZnS QDs was nontoxic in

comparison with some traditional QDs. Moreover, the hybrid system of Mn:ZnS QDs combined with Fenton reaction presented a simple and feasible strategy to solve the discrimination and detection of different metal species.

Acknowledgements

We are grateful for the financial support from the National Natural Science Foundation of China (21375095, 20975054), the Tianjin Natural Science Foundation (12JCZDJC21700), the Foundation for the Author of National Excellent Doctoral Dissertation of PR China (FANEDD-201023), the Program for Innovative Research Team in University of Tianjin (TD12-5038) and Program for young backbone talents in Tianjin (ZX110GG015).

Notes and references

1 D. J. Williams, C. Critchley, S. Pun, M. Chaliha, T. J. O'Hare, *J. Agric. Food Chem.*, 2010, **58**, 8512-8521.

2 H. H. Yin, H. Kuang, L. Q. Liu, L. G. Xu, W. Ma, L. B. Wang, C. L. Xu, *ACS Appl. Mater. Interfaces*, 2014, **6**, 4752-4757.

3 S. P. Jia, M. M. Liang, L. H. Guo, *J. Phys. Chem. B*, 2008, **112**, 4461-4464.

4 Y. M. Zhang, Y. Chen, Z. Q. Li, N. Li, Y. Liu, *Bioorg. Med. Chem.*, 2010, **18**, 1415–1420.

5 Y. H. Zhang, Y. M. Zhang, Y. Chen, Y. Yang, Y. Liu, *Org. Chem. Front.*, 2014, **1**, 355-360.

6 H. Kim, Y. J. Na, E. J. Song, K. B. Kim, J. M. Bae, C. Kim, *RSC Adv.*, 2014, **4**, 22463-22469.

7 E. L. Que, D. W. Domaille, C. J. Chang, *Chem. Rev.*, 2008,**108**, 1517-1549.

8 D. C. Crans, K. A. Woll, K. Prusinskas, M. D. Johnson, E. Norkus, *Inorg. Chem.*, 2013, **52**, 12262-12275.

9 S. T. Moin, T. S. Hofer, A. B. Pribil, B. R. Randolf, B. M. Rode, *Inorg. Chem.*, 2010, **49**, 5101-5106.

10 Z. Yang, M. Y. She, B. Yin, J. H. Cui, Y. Z. Zhang, W. Sun, J. L. Li, Z. Shi, *J. Org. Chem.*, 2012, **77**, 1143-1147.

11 D. J. Goss, E. C. Theil, *Acc. Chem. Res.*, 2011, **44**, 1320-1328.

12 T. L. Foster, J. P. Caradonna, *J. Am. Chem. Soc.*, 2003, **125**, 3678-3679.

13 S. P. Wu, Y. P. Chen, Y. M. Sung, *Analyst*, 2011, **136**, 1887-1891.

14 D. J. R. Lane, D. R. Richardson, *Free Radic. Biol. Med.*, 2014, **75**, 69-83.

15 J. E. T. Andersen, *Analyst*, 2005, **130**, 385-390.

16 C. M. G. van den Berg, *Anal. Chem.*, 2006, **78**, 156-163.

17 R. K. Pathak, J. Dessingou, V. K. Hinge, A. G. Thawari, S. K. Basu, C. P. Rao, *Anal. Chem.*, 2013, **85**, 3707-3714.

18 C. X. Yang, H. B. Ren, X. P. Yan, *Anal. Chem.*, 2013, **85**, 7441-7446.

19 M. Wang, J. G. Wang, W. J. Xue, A. X. Wu, *Dyes Pigment*, 2013, **97**, 475-480.

20 K. G. Qu, J. S. Wang, J. S. Ren, X. G. Qu, *Chem. Eur. J.*, 2013, **19**, 7243-7249.

21 C. M. Wansapura, C. J. Seliskar, W. R. Heineman, *Anal. Chem.*, 2007, **79**, 5594-5600.

22 Y. F. Huang, Y. W. Lin, H. T. Chang, *Langmuir*, 2007, **23**, 12777-12781.

23 P. Wu, Y. Li, X. P. Yan, *Anal. Chem.*, 2009, **81**, 6252-6257.

24 H. B. Ren, B. Y. Wu, J. T. Chen, X. P. Yan, *Anal. Chem.*, 2011, **83**, 8239-8244

25 K. Ding, L. H. Jing, C. Y. Liu, Y. Hou, M. Y. Gao, *Biomaterials*, 2014, **35**, 1608-1617.

26 I. Sánchez-Barragán, J. M. Costa-Fernández, M. Valledor, J. C. Campo, A. Sanz-Medel, *Trends Anal. Chem.*, 2006, **25**, 958-967.

27 Y. He, H. F. Wang, X. P. Yan, *Anal. Chem.*, 2008, **80**, 3832-3837.

28 J. M. Traviesa-Alvarez, I. Sánchez-Barragán, J. M. Costa-Fernández, R. Pereiro, A. Sanz-Medel, *Analyst*, 2007, **132**, 218–223.

29 H. F. Wang, Y. Y. Wu, X. P. Yan, *Anal. Chem.*, 2013, **85**, 1920-1925.

30 P. Wu, Y. He, H. F. Wang, X. P. Yan, *Anal. Chem.*, 2010, **82**, 1427-1433.

31 E. Sotelo-Gonzalez, M. T. Fernandez-Argüelles, J. M. Costa-Fernandez, A. Sanz-Medel, *Anal. Chim. Acta*, 2012, **712**, 120-126.

32 W. S. Zou, D. Sheng, X. Ge, J. Q. Qiao, H. Z. Lian, *Anal. Chem.*, 2011, **83**, 30-37.

33 H. Yan, H. F. Wang, *Anal. Chem.*, 2011, **83**, 8589-8595.

34 P. Wu, T. Zhao, S. L. Wang, X. D. Hou, *Nanoscale*, 2014, **6**, 43–64.

35 X. Zeng, A. T. Lemley, *J. Agric. Food Chem.*, 2009, **57**, 3689-3694.

36 M. M. Liang, S. P. Jia, S. C. Zhu, L. H. Guo, *Environ. Sci. Technol.*, 2008, **42**, 635-639.

37 J. H. Chung, C. S. Ah, D. J. Jang, *J. Phys. Chem. B.*, 2001, **105**, 4128-4132.

38 H. J. H. Fenton, *J. Chem. Soc., Trans.*, 1894, **65**, 899-911.

39 Z. H. Qi, P. M. de Molina, W. Jiang, Q. Wang, K. Nowosinski, A. Schulz, M. Gradzielski, C. A. Schalley, *Chem. Sci.*, 2012, **3**, 2073-2082.

40 M. Shahid, T. McCarthy-Ward, J. Labram, S. Rossbauer, E. B. Domingo, S. E. Watkins, N. Stingelin, T. D. Anthopoulos, M. Heeney, *Chem. Sci.*, 2012, **3**, 181-185.

41 K. S. Kasprzak, *Free Radic. Biol. Med.*, 2002, **32**, 958–967.

42 S. R. Taylor, S. M. McLennan, in the *continental crust*, its composition and evolution, Blackwell Scientific Publications, New York, 1999; pp. 15-16.

43 K. Sauer, H. Scheer, P. Sauer, *Photochem. Photobiol.*, 1987, **46**, 427–440.

44 H. Q. Chen, J. C. Ren, *Analyst*, 2012, **137**, 1899-1903

45 Y. Lu, B. Yan, J. L. Liu, *Chem. Commun.*, 2014, **50**, 9969—9972.

46 W. T. Huang, W. Y. Xie, Y. Shi, H. Q. Luo, N. B. Li, *J. Mater. Chem.*, 2012, **22**, 1477-1481

47 S. K. Poznyak, D. V. Talapin, E. V. Shevchenko, H. Weller, *Nano Lett.*, 2004, **4**, 693–698.

48 Y, Zhang, Y. Li, X. P. Yan, *Anal. Chem.*, 2009, **81**, 5001–5007.

49 X. P. Yan, M. J. Hendry, R. Kerrich, *Anal. Chem.*, 2000, **72**, 1879–1884.